Cellulose (2010) 17:69–81
DOI 10.1007/s10570-009-9380-3

Glucomannan composite films with cellulose nanowhiskers

Kirsi S. Mikkonen · Aji P. Mathew · Kari Pirkkalainen · Ritva Serimaa · Chunlin Xu · Stefan Willför · Kristiina Oksman · Maija Tenkanen

Received: 8 June 2009 / Accepted: 9 November 2009 / Published online: 21 November 2009

Abstract Spruce galactoglucomannans (GGM) and konjac glucomannan (KGM) were mixed with cellulose nanowhiskers (CNW) to form composite films. Remarkable effects of CNW on the appearance of the films were detected when viewed with regular and polarizing optical microscopes and with a scanning electron microscope. Addition of CNW to KGM-based films induced the formation of fiberlike structures with lengths of several millimeters. In GGM-based films, rodlike structures with lengths of several tens of micrometers were formed. The degree of crystallinity of mannan in the plasticized KGM-based films increased slightly when CNW were added, from 25 to 30%. The tensile strength of the KGM-based films not containing glycerol increased with increasing CNW content from 57 to 74 MPa, but that of glycerol-plasticized KGM and GGM films was not affected. Interestingly, the notable differences in the film structure did not appear to be related to the thermal properties of the films.

Keywords Composites · Cellulose nanowhiskers · Films · Konjac glucomannan · Spruce galactoglucomannans

K. S. Mikkonen (✉) · M. Tenkanen
Department of Applied Chemistry and Microbiology, University of Helsinki, P.O. Box 27, 00014 Helsinki, Finland
e-mail: kirsi.s.mikkonen@helsinki.fi

K. S. Mikkonen
Department of Food Technology, University of Helsinki, P.O. Box 66, 00014 Helsinki, Finland

A. P. Mathew · K. Oksman
Division of Manufacturing and Design of Wood and Bionanocomposites, Luleå University of Technology, 97187 Luleå, Sweden

K. Pirkkalainen · R. Serimaa
Department of Physics, University of Helsinki, P.O. Box 64, 00014 Helsinki, Finland

C. Xu · S. Willför
Process Chemistry Centre, Åbo Akademi University, Åbo, Porthansgatan 3, 20500 Turku, Finland

Present Address:
C. Xu
School of Biotechnology, Royal Institute of Technology (KTH), AlbaNova University Centre, 10691 Stockholm, Sweden

Introduction

O-acetyl galactoglucomannans (GGM) are polysaccharides that can be obtained as a by-product from thermomechanical pulping of Norway spruce (*Picea abies*) at high yield and purity (Willför et al. 2003). Use of GGM as bio-based and biodegradable oxygen barrier film former was suggested and the cost of such films was estimated to be approximately nine times lower than that of the widely used synthetic oxygen

barrier material ethylene vinyl alcohol (Persson et al. 2007). The formation of cohesive films from GGM requires the use of an external plasticizer, such as glycerol (Hartman et al. 2006). However, even with glycerol, the mechanical properties of GGM films have previously been considered to be poor (Mikkonen et al. 2008).

GGM consist of a backbone of β-1,4-D-mannopyranosyl and β-1,4-D-glucopyranosyl units carrying single α-D-galactopyranosyl residues 1,6-linked to mannose units, and acetyl substituents attached to the C-2 or C-3 positions of mannose (Sjöström 1993). The ratio of mannose:glucose:galactose of water-extracted GGM is approximately 4:1:0.5, the degree of acetylation is about 20–30%, and the molar mass varies from approximately 30000 to 60000 g/mol (Willför et al. 2008). Konjac glucomannan (KGM), a polysaccharide from the tuber of *Amorphophallus konjac*, has a chemical composition rather similar to that of GGM with a mannose:glucose ratio of 1.6:1 and a degree of acetylation of 5% (Takigami 2000). The molar mass of KGM is significantly higher than that of GGM, approximately 1000000 g/mol (Li et al. 2006a). In contrast to GGM, KGM shows excellent film formation with high tensile strength and elongation at break (Cheng et al. 2006). These properties were further enhanced by blending KGM with other polymers (Xiao et al. 2001; Li et al. 2006b).

Cellulose nanowhiskers (CNW) have been studied as reinforcements of various synthetic and some natural polymer matrices (Samir et al. 2005; Kvien et al. 2007; Petersson et al. 2007; Saxena et al. 2009). CNW are prepared by acid hydrolysis of cellulose, which yields a suspension of highly crystalline, nanoscale (width approximately 10 nm, length several hundreds of nm), whisker-shaped rods in water, the dimensions of which are dependent on the cellulose origin and the hydrolysis conditions (de Souza Lima and Borsali 2004). The crystalline structures are extremely tightly packed and tend to be impermeable to gases (McHugh and Krochta 1994). Due to the extensively ordered structure, the tensile strength of CNW is high (Samir et al. 2005). Uniform dispersion of the reinforcement leads to large interfacial areas between the reinforcement and matrix, which alters the molecular mobility, relaxation behavior, and the thermal, mechanical, and gas barrier properties of the nanocomposite (Sorrentino et al. 2007). When reinforcement-reinforcement interactions are favored, nanocomposites containing CNW can have greatly improved mechanical properties in comparison to the matrix polymer alone. However, high matrix-reinforcement interactions, such as transcrystallization, can result in low mechanical performance (Samir et al. 2005). The tensile properties of a starch-CNW system were dependent on CNW content, moisture conditions, and the type of plasticizer (Anglès and Dufresne 2001; Lu et al. 2006; Mathew et al. 2008). The properties of CNW-reinforced xylan films also depended on the method of CNW preparation (Saxena et al. 2009). In the present study, CNW were used as a reinforcement in GGM- and KGM-based films. The morphology of the films as well as their tensile and thermal properties were studied.

Experimental part

Materials

GGM was obtained from an industrial-scale isolation trial from process water of a Finnish pulp mill, according to the method developed by Willför et al. (2003). The concentrated solution was spray-dried and then dissolved in water at 10 g L^{-1}, filtered through a fiberglass filter to remove a small amount of agglomerated particles, concentrated using a rota evaporator, and vacuum-dried. The molar mass of GGM was determined by multiangle laser light scattering to be 39000 g/mol according to Xu et al. (2009). The amorphous mannan reference for X-ray study was obtained by purifying GGM with dialysis against water and lyophilizing (Laine et al., submitted). This sample had no long range order in atomic arrangement on the basis of the diffraction pattern. KGM (Luxara 208-1, purity 80–85 wt%) was kindly provided by Arthur Branwell & Co. Ltd. (Epping, Essex, UK). The CNW were prepared from microcrystalline cellulose (Vivapur 105: JRS Pharma GmbH & Co KG, Rosemberg, Germany) by sulphuric acid hydrolysis, according to Bondenson et al. (2006). Glycerol (101184 K) was obtained from BDH Laboratory Supplies (Lutterworth, Leicestershire, UK).

Preparation of films

The films were prepared from GGM and KGM alone and at GGM:CNW and KGM:CNW ratios of 95:5 and 85:15 (w/w). The GGM-based films were plasticized using glycerol at 40% (wt% of GGM and cellulose). From KGM, the films were prepared with 40% glycerol and without added plasticizer. The mannans were dissolved in deionized water at 80 °C, preceding the addition of CNW when used. The mannan-CNW suspensions were mixed by magnetic stirring at 80 °C for 5 min, after which glycerol was added when used. The combined content of GGM and CNW in the film suspensions was 10 g L^{-1}, and that of KGM and CNW was 5 g L^{-1}, due to the high viscosity of KGM in water. Air was removed by ultrasonication under vacuum, after which 80 mL of suspensions containing GGM were cast on Teflon plates (diameter 13 cm) and 100 mL of suspensions containing KGM were cast on Petri dishes (diameter 14 cm) to obtain films with average thicknesses of approximately 80 and 40 μm, respectively. The films were dried overnight at 60 °C and stored in desiccators containing saturated $Mg(NO_3)_2$ or NaCl solutions to condition the films to relative humidities (RHs) of 54 and 76%, respectively, for water content analysis. Other analyses were done on films conditioned at 54% RH.

Microscopy

Optical imaging of the films was done with a Leica Dialux 20 optical microscope (OM) (Leica Microsystems GmbH, Wetzlar, Germany) and a Zeiss PolJenalab polarizing OM (Carl Zeiss Inc., Oberkochen, Germany), using transmitted light. The fractured surfaces of the films were viewed with scanning electron microscopy (SEM). Rectangular strips of approximately 5 mm × 40 mm were plunged into liquid nitrogen and fractured manually using tweezers. The fractured fragments were mounted on aluminum stubs, using conductive carbon tape, and coated with a thin layer of gold by direct-current sputtering. Images of the oriented fracture faces were collected, using a Jeol JSM 840A SEM (Jeol Ltd., Tokyo, Japan) operated under high vacuum, using the secondary electron-imaging mode.

X-ray diffraction

All films and oven-dried (at 60 °C) CNW were characterized using X-ray diffraction. Wide-angle X-ray-scattering measurements were carried out in perpendicular transmission geometry using Cu $K\alpha_1$ radiation. A setup with a Rigaku rotating anode (fine focus) X-ray tube (Rigaku Corp., Tokyo, Japan) and an MAR345 image plate detector (Rayonix, Evanston, IL, USA) was used. The beam was monochromated and focused on the detector with a bent Si(111) crystal and a totally reflecting mirror. The intensities measured were corrected for absorption of radiation and a geometrical factor to compensate for the flat detector. The angular range was calibrated with silver behenate, silicon, aluminum, and sodium chloride standards. The broadening of the diffraction maxima due to the instrument was determined to be 0.37° at 2θ of 31.6°, using the 200 reflection of NaCl.

The diffraction patterns were measured at 31 °C (304 K) and 60 °C (333 K). The samples were heated in situ under ambient atmosphere with a Linkam heating stage (Linkam Scientific Instruments, Tadworth, Surrey, UK). The heating was started at 304 K and the temperature was raised to 333 K with a gradient of 10 K min^{-1}. After heating, a 10-min pause was kept to ensure an isotropic distribution of heat in the sample. In each temperature step the diffraction pattern was cumulated for 20 min.

The scattering angles are in 2θ, which is twice the value of the Bragg angle in Bragg's law $\lambda = 2d_{hkl}\sin(\theta\ [^\circ])$, or in wavelength-invariant form $q = 2\pi/d_{hkl} = 4\pi\ \sin(\theta)/\lambda$ [1/Ångsröm]. In these formulas, θ is the Bragg angle, λ the wavelength of the radiation used, and d_{hkl} the distance of the planes given by Miller indices *hkl*.

X-ray diffraction patterns measured at 60 °C were used in the determination of mannan crystallinity in the samples. The scattering of X-rays due to the CNW content in the samples was first subtracted from the measured diffraction patterns, so that the subtracted diffraction patterns would only consist of scattering from the mannan. The pure CNW diffraction pattern used in the subtraction was recorded from the oven-dried CNW sample of approximately the same thickness as the mannan samples.

The 100% crystalline mannan diffraction pattern was calculated using the known crystal structure and atomic coordinates of mannan I (Atkins et al. 1988).

The positions, intensities, and widths of all the reflections of mannan I in the angular range of 5°–60° were calculated, using PowderCell 2.4 computer software (Institute for Molecules and Materials, Radboud University Nijmegen, Nijmegen, The Netherlands) (Kraus and Nolze 1996). The fully amorphous mannan diffraction pattern was measured from the pure mannan powder sample, which is assumed to have a crystallinity of 0% (i.e. all the crystallinity estimations are crystallinities compared to this reference). The amorphous reference was also measured at 60 °C.

The 100% crystalline mannan diffraction pattern and the amorphous background were fitted with the least-squares method to the measured diffraction pattern and the crystallinity of mannan in the samples was determined from the best fit of the relative amount of crystalline and amorphous components. The uncertainties due to the fitting method were estimated by varying slightly the fitting parameters and calculating the effect of the changes on the calculated crystallinity values. The uncertainties also include the possibility that the samples contain crystalline mannan II, which is not taken into account in the crystallinity calculations.

Thermal gravimetric analysis (TGA)

The thermal degradation of the materials and films used was studied in triplicate, using a TGA Q500 (TA Instruments, New Castle, DE, USA). For this purpose, the CNW suspension was dried at 60 °C overnight, as were the films. The dried CNW, glycerol, and KGM and GGM powders were conditioned at 54% RH for at least 3 d before analysis. The samples were heated from 21 to 600 °C at a rate of 5 °C min^{-1} and the sample weight was recorded. A Mettler-Toledo TGA 850 thermogravimetric analyzer (Mettler-Toledo AG, Greifensee, Switzerland) equipped with STAR^e software (Star Software Systems, Warner Robins, GA, USA), was used to determine the water content of the films. Three replicate specimens of each film were heated from 25 to 120 °C at a heating rate of 50 °C min^{-1}. The temperature was then maintained at 120 °C for 10 min, during which a steady specimen weight was reached. Weight loss during the heat treatment was taken as water content.

Mechanical testing

Dynamic mechanical analysis (DMA) of films was performed on a DMA Q800 (TA Instruments), using a film tension clamp. Triplicate specimens of 5 mm × 30 mm were prepared. The specimen width was measured with a digital caliper (NSK Ltd., Tokyo, Japan), and the thickness was determined as an average of three measurements with a Lorenzen & Wettre micrometer (Lorenzen & Wettre, Kista, Sweden) at 1-μm precision. The gap between the jaws at the beginning of the test was 14 mm. A strain of 0.1% was applied on KGM-based films and a strain of 0.05% on GGM-based films. A frequency of 1 Hz was used. The specimens were equilibrated at −120 °C for 5 min, after which the storage modulus (E'), loss modulus (E''), and loss tangent (tan δ) were determined as a function of temperature from −120 to 100 °C at a heating rate of 5 °C min^{-1}.

The tensile strength, elongation at break, and Young′s modulus of the films were determined, using an Instron 4411 mechanical property tester with a 500-N load cell (Instron Ltd., Norwood, MA, USA). The initial grip distance was 25 mm and the rate of grip separation was 5 mm min^{-1}. Two films of each type and 5–7 specimens from each film were tested. The specimens were 6 mm wide and approximately 80 mm long. The thickness of the specimens was measured at three points, using a micrometer (NSK, Japan) at 10-μm precision and an average was calculated.

Results

Microscopy

When examined visually, the KGM-based films without CNW were clear and transparent. However, OM showed the presence of some irregularly shaped agglomerates that could have originated from less soluble fractions of KGM (Fig. 1a). Addition of CNW caused a remarkable change in the appearance of the films, which was seen immediately after drying of the films. The CNW induced the formation of fibrous structures visible with the naked eye and also shown by OM (Fig. 1b). The appearance of the KGM films and KGM-CNW composites was similar, regardless of the use of glycerol. In addition, the

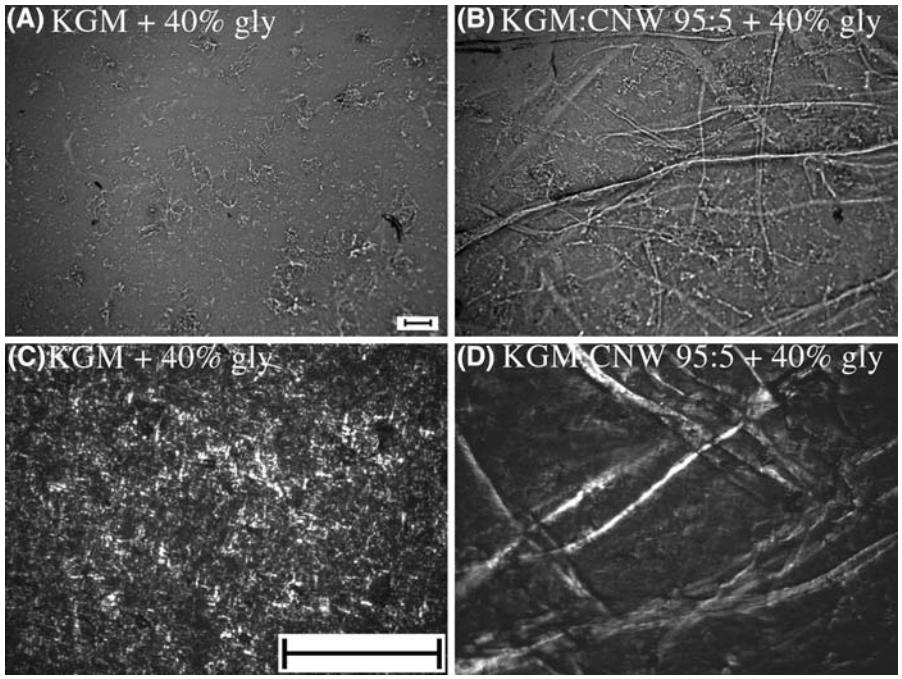

Fig. 1 Optical microscopic images of films from (**a**) KGM and (**b**) KGM:CNW 95:5 (weight ratio) plasticized with 40% glycerol (gly) (wt% of KGM and CNW) and polarizing optical microscopic images of films from (**c**) KGM and (**d**) KGM:CNW 95:5 plasticized with 40% glycerol. The scale bar in **a** is 0.1 mm and images **a** and **b** are at the same magnification. The scale bar in **c** is 1 mm and images **c** and **d** are at the same magnification

KGM:CNW ratio did not affect the appearance of the composites. The fibrous structures were not orientated, but ran randomly in all directions along the film plane.

Polarizing OM confirmed the extraordinary effect of the CNW on the structure of the KGM-based films. The bright components seen with polarizing OM were visible due to their characteristic of orientating polarized light, which indicates crystalline structures. In the films from pure KGM, the crystalline structures were seen as single, relatively small, bright spots scattered all over the films (Fig. 1c). The KGM films containing glycerol had a higher number of structures visible with polarizing OM than the unplasticized films. In the KGM-CNW composites, the bright components were organized as long and fibrous structures resembling those seen with regular OM (Fig. 1d).

The CNW also clearly altered the structure of the GGM-based films. The OM study of the GGM-CNW composites showed the presence of rods with lengths of tens of micrometers (Fig. 2a), which were absent in the film from pure GGM. When viewed with polarizing OM, the film from pure GGM showed some poorly visible bright spots several micrometers in size (not shown), but the GGM-CNW composites contained bright rods corresponding to the structures seen with regular OM (Fig. 2b). The size of the polarizing structures increased with increasing content of the CNW, indicating that the structures most probably originated from the CNW.

The differences in the film structures were also seen with SEM. The films from the pure mannans had relatively smooth fractured surfaces (Fig. 3a, d, and g). The effect of the CNW was seen as increased heterogeneity of the film. The layered structure of the KGM-CNW composites viewed with SEM (Fig. 3b, c, e, and f) may correspond to the fibrous shapes visible with the naked eye and with OM. In the GGM-based films, the increase in CNW content caused increasing porosity.

X-ray diffraction

Figure 4 shows the X-ray diffraction patterns of unplasticized and plasticized KGM:CNW 85:15

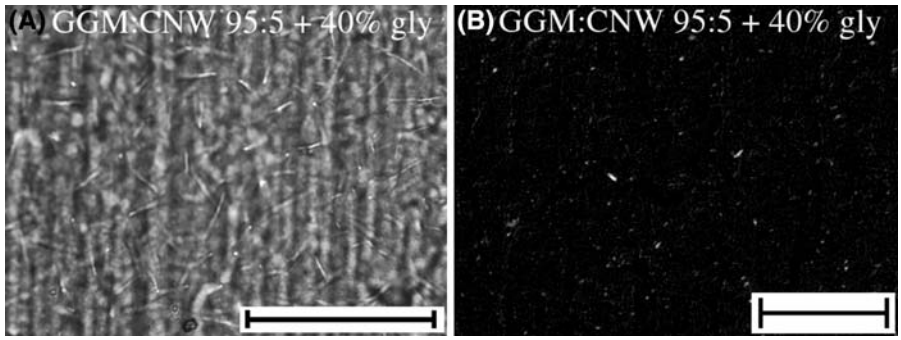

Fig. 2 **a** Optical microscopic image and (**b**) polarizing optical microscopic image of film from GGM:CNW 95:5 (weight ratio) plasticized with 40% glycerol (gly) (wt% of GGM and CNW). The scale bars are 0.1 mm. The vertical texture in **a** is due to the texture of the Teflon plates

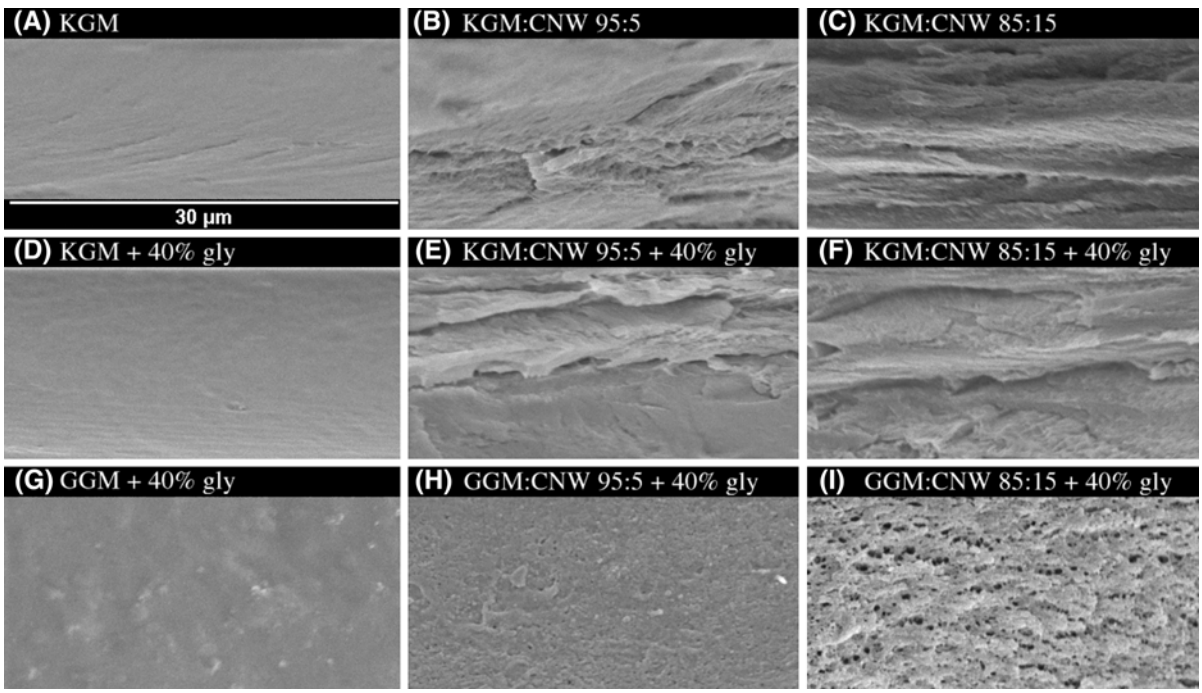

Fig. 3 Scanning electron micrographs of cross-sections of unplasticized films from (**a**) KGM, (**b**) KGM:CNW 95:5, and (**c**) KGM:CNW 85:15 and of films from (**d**) KGM (**e**) KGM:CNW 95:5, and (**f**) KGM:CNW 85:15, (**g**) GGM, (**h**) GGM:CNW 95:5, and (**i**) GGM:CNW 85:15 plasticized with 40% glycerol (gly) (wt% of mannan and CNW). All images are at the same magnification

composite films, from which the diffraction of cellulose has been subtracted. The degrees of crystallinity of mannan in the films calculated from the X-ray diffraction patterns are shown in Table 1. The unplasticized KGM:CNW 85:15 composite film had the lowest degree of mannan crystallinity, 11.8%. The degree of mannan crystallinity of the plasticized KGM and GGM composite films was clearly higher, close to 30 and 25%, respectively. The addition of CNW slightly increased the crystallinity of mannan in the plasticized KGM films. An upper boundary for the average size of the mannan crystallites was calculated with the Scherrer formula (Guinier 1994); the value was 3.5 nm (i.e. the average size of the

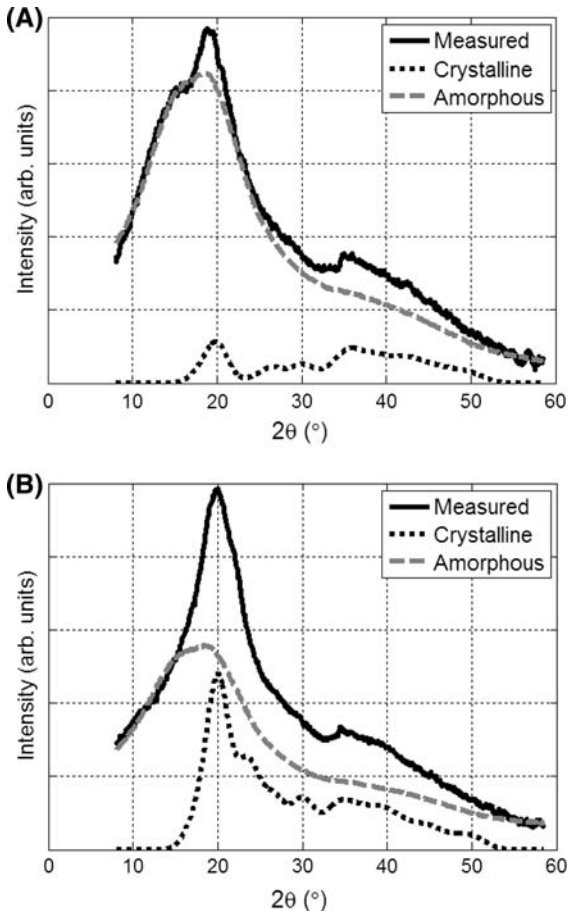

Fig. 4 X-ray diffraction patterns and crystallinity fits of (**a**) unplasticized and (**b**) plasticized KGM:CNW 85:15 composite films. The diffraction from cellulose has been subtracted from the measured curve

Table 1 Degree of crystallinity of mannan in the films measured at 60 °C

Film	Crystallinity of mannan (%)
KGM	13.3 ± 2.4
KGM:CNW 95:5	13.1 ± 2.5
KGM:CNW 85:15	11.8 ± 2.7
KGM + 40% glycerol	24.7 ± 1.5
KGM:CNW 95:5 + 40% glycerol	30.9 ± 1.9
KGM:CNW 85:15 + 40% glycerol	29.3 ± 1.6
GGM + 40% glycerol	24.3 ± 1.2
GGM:CNW 95:5 + 40% glycerol	25.2 ± 1.8
GGM:CNW 85:15 + 40% glycerol	26.6 ± 1.7

mannan crystallites is smaller than 3.5 nm). The CNW used in this study included approximately 11 wt% of a crystalline impurity of unknown origin. The impurity was discovered from unexpected maxima in the X-ray diffraction patterns of all the samples containing CNW, including the pure CNW sample. The positions of these maxima were at 19.2° (1.346 1/Å) and 23.3° (1.643 1/Å), which did not correspond to any known crystalline arrangement of cellulose. The unexpected maxima disappeared from the diffraction patterns when the samples were heated to 60 °C, so this temperature was used for determination of the degree of mannan crystallinity. The small amount of the impurity in the CNW was considered insignificant for the film properties.

Thermal stability and water content

To study the thermal degradation of the raw materials and films, the specimens were heated to 600 °C, using a TGA (Fig. 5). The loss of water was seen close to 100 °C. During further heating, the thermal degradation of glycerol began at temperatures higher than 120 °C. The KGM and GGM powders had higher thermal degradation stability than the glycerol and CNW (Fig. 5a).

Those KGM-based films not containing glycerol maintained their weight until higher temperatures were reached than those of the glycerol-plasticized films. Their thermal degradation began steeply at approximately 250 °C, whereas that of the glycerol-plasticized KGM- and GGM-based films was initiated between 100 and 150 °C and took place more gradually. The TGA curves of the KGM-based films not containing glycerol were almost identical up to approximately 280 °C, regardless of the use of CNW, after which the films with the CNW were degraded somewhat more rapidly up to about 400 °C (Fig. 5b). When glycerol was used, the addition of the CNW at a KGM:CNW ratio of 95:5 slightly increased the degradation stability of the KGM-based films (Fig. 5c). The glycerol-pasticized KGM:CNW 85:15 composite had a lower degradation stability and a TGA curve of somewhat different shape than the corresponding composite at a ratio of 95:5 and the pure KGM-based film. The degradation stability of the pure GGM-based film and of the composite at the GGM:CNW ratio of 95:5 were also slightly higher than that of the GGM:CNW 85:15 composite (Fig. 5d).

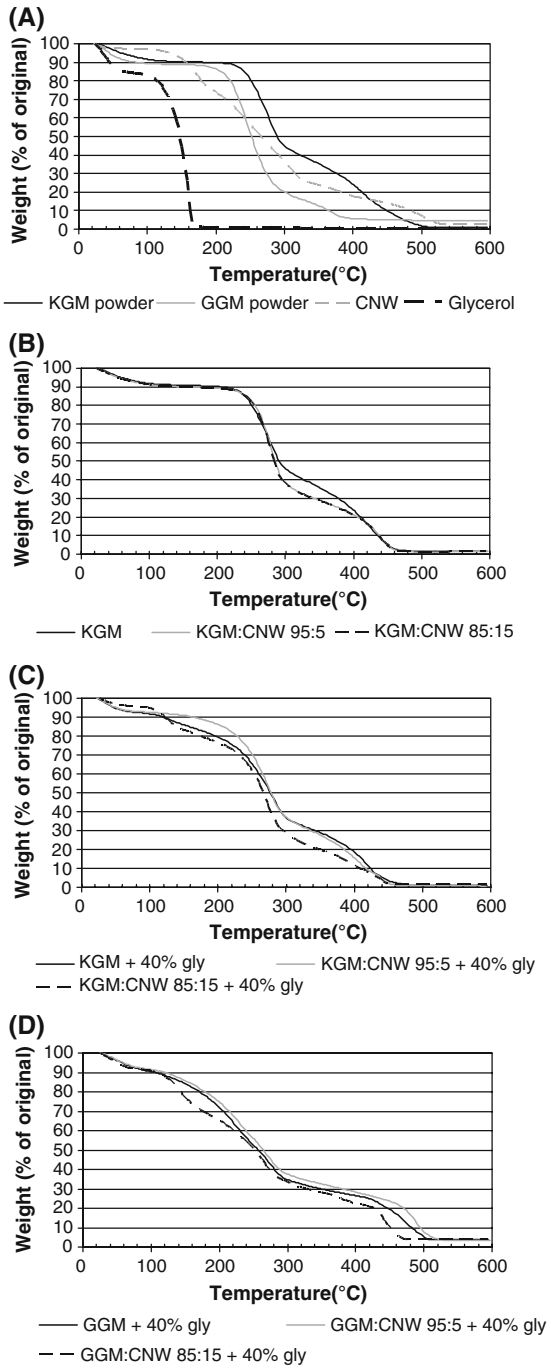

Fig. 5 Selected representative thermal gravimetric analysis graphs of (**a**) raw materials used and films from (**b**) unplasticized KGM and KGM:CNW at weight ratios of 95:5 and 85:15, (**c**) KGM and KGM:CNW at weight ratios of 95:5 and 85:15 plasticized with 40% glycerol (gly) (wt% of KGM and CNW), and (**d**) GGM and GGM:CNW at weight ratios of 95:5 and 85:15 containing 40% glycerol (wt% of GGM and CNW). All specimens were conditioned at 54% RH before analysis

In addition to thermal degradation stability, the water content of the films was studied, using TGA. The results are indicative, because the thermal degradation study showed that the degradation of films with a mannan:CNW ratio of 85:15 containing 40% glycerol was initiated at approximately 110 °C, whereas the water content study was done until 120 °C. The latter temperature used was previously considered suitable for films not containing CNW (Mikkonen et al. 2007).

When conditioned at 54% RH, the water content of the films varied from 7.6 to 11.8% (Table 2). Those KGM-based films not containing glycerol had the lowest water content, and the GGM-based films that were plasticized with 40% glycerol had the highest. The water content at 54% RH did not show a clear dependence on the amount of CNW. In contrast, the water content at 76% RH generally decreased with increasing amounts of CNW, especially with the GGM-based films. The film from GGM had a water content of 22%, whereas that of the GGM:CNW 85:15 film was only 15%. In a manner similar to that at 54% RH, the KGM films not containing glycerol absorbed the least water.

Mechanical properties

The plasticizing effect of glycerol can be seen in the shape of the storage modulus (E′) curve (Fig. 6a and b). The E′ of the KGM-based films not containing glycerol decreased during heating, but did not show a well-defined transition zone (Fig. 6a). The glycerol-plasticized KGM and GGM films showed a clear decrease in E′ (Fig. 6b and c), and a peak in E″ (results not shown) and in tan delta (Fig. 7) at approximately −50 °C, indicating α-relaxation. The dynamic mechanical behavior of the mannan-CNW composites at both ratios studied was similar to those of the corresponding films from KGM and GGM not containing CNW (Figs. 6 and 7). To eliminate the effect of variation in thickness of the films and the error in its measurement, the E′ in Fig. 6 was normalized at 1 GPa, as explained by Mathew et al. (2008).

The tensile strength of the KGM-based films not containing glycerol increased with increasing CNW content (Fig. 8a). However, the CNW did not significantly affect the other tensile properties of these films. The tensile strength and Young′s modulus of

Table 2 Water content of mannan-CNW films. The averages are based on three measurements

Film	Water content (±sd) (wt%)	
	RH 54%	RH 76%
KGM	8.2 ± 0.6	12.6 ± 1.0
KGM:CNW 95:5	9.9 ± 0.8	13.9 ± 1.4
KGM:CNW 85:15	7.6 ± 0.4	10.7 ± 0.6
KGM + 40% glycerol	10.8 ± 1.2	19.9 ± 0.6
KGM:CNW 95:5 + 40% glycerol	10.2 ± 0.3	18.5 ± 0.4
KGM:CNW 85:15 + 40% glycerol	10.7 ± 1.0	18.2 ± 0.4
GGM + 40% glycerol	11.8 ± 0.6	21.6 ± 0.3
GGM:CNW 95:5 + 40% glycerol	10.7 ± 0.4	16.1 ± 0.4
GGM:CNW 85:15 + 40% glycerol	11.8 ± 0.6	14.6 ± 0.3

the KGM-based films decreased and the elongation at break increased when glycerol was added, as expected (Fig. 8). The GGM-based films, plasticized with glycerol, had significantly lower tensile strength and elongation at break than the KGM-based films, but their Young′s moduli were rather similar to those of the glycerol-plasticized KGM-based films. Surprisingly, the addition of CNW showed no clear effect on the tensile properties of the plasticized KGM and GGM films.

Discussion

Effect of CNW on morphology of films

The addition of CNW greatly changed the appearance of the KGM-based films. This could be seen even with the naked eye and was confirmed with microscopy. The visible structures in the composites were several magnitudes larger than the size of the CNW. Chanzy et al. showed that glucomannan can crystallize on cellulose microfibrils, which, however, are much longer than CNW (Chanzy et al. 1982). To the best of our knowledge, structures of similar size have not been reported previously in films from other polymers with CNW. Microscopic study with OM and SEM showed that CNW also induced morphological changes in GGM-based films. The structures formed in the GGM-CNW composites were considerably smaller than those in the KGM-CNW composites. This was most likely affected by the lower molar mass of GGM compared with KGM. The pores seen in the GGM-CNW films with SEM could have been derived from air bubbles, pulled-out undissolved structures and/or moisture evaporation during film drying and the sputtering operation (Nordqvist et al. 2007).

Polarizing OM imaging suggested that the formation of the fibrous and rodlike structures was due to reorganization of crystalline components in the films. As found with the X-ray diffraction measurements, the pure KGM- and GGM-based films were semicrystalline. The degree of crystallinity of mannan of the KGM films was higher when glycerol was used, which could also be seen with polarizing OM. Surprisingly, the crystalline structures in those GGM films not containing CNW detected with X-ray diffraction were poorly visible with polarizing OM. This could have been due to the small size of crystalline structures in the GGM films. The degree of crystallinity of mannan in the plasticized KGM-based films slightly increased when CNW were added. However, the differences in the degree of crystallinity of mannans due to the addition of CNW were small and did not correspond to the remarkable differences in the visual appearance of the films. Therefore, increased mannan crystallization could not have been responsible for the formation of the fibrous structures. In contrast, mannans could gather CNW into larger crystalline structures visible with polarizing OM.

When conditioned at 76% RH, the water content of the films containing CNW was lower than that of films from pure mannans, especially for GGM films. Due to the plasticizing effect of water, the molecular mobility of polysaccharides and their ability to rearrange to crystalline forms increase at high levels of RH.

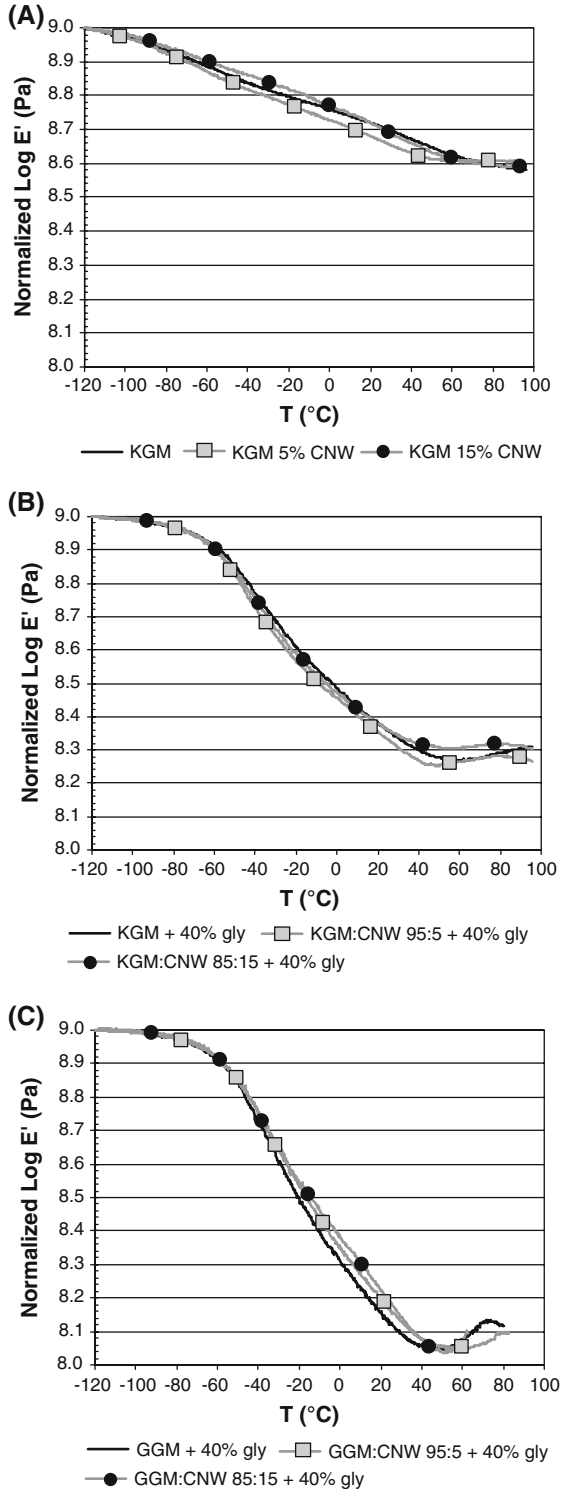

◀**Fig. 6** Logarithm of the selected representative storage modulus (E′) spectra of KGM-based films (**a**) without and (**b**) with 40% glycerol (wt% of KGM and CNW) as plasticizer and (**c**) GGM-based films with 40% glycerol. The measurement points in (**c**) above 60 °C are missing because most of the GGM-based film specimens broke during measurement at 60–80 °C. The E′ at −120 °C was normalized at 1 GPa for all the samples

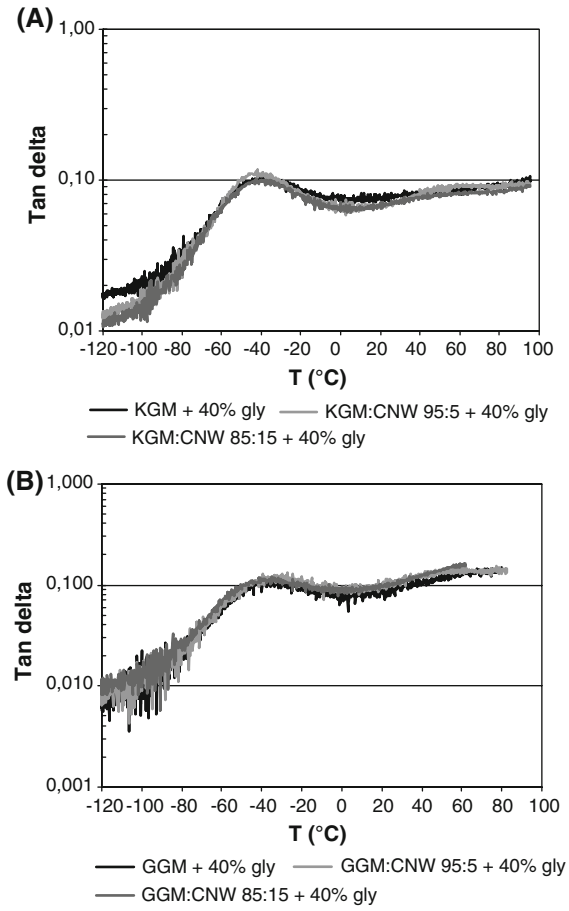

Fig. 7 Selected representative tangent delta spectra of (**a**) KGM- and (**b**) GGM-based films plasticized with 40% glycerol (wt% of mannans and CNW)

This could further lead to tightly packed molecular structures, and therefore to a decreased ability to absorb water (Anglès and Dufresne 2000). The results of the water content analysis suggest that at 76% RH, the interactive effect of the CNW and high RH increased the level of crystallization in the films.

Effect of CNW on thermal and mechanical properties

Unexpectedly, the remarkable differences in the film structure did not indicate great changes in the other film properties studied. The thermal degradation

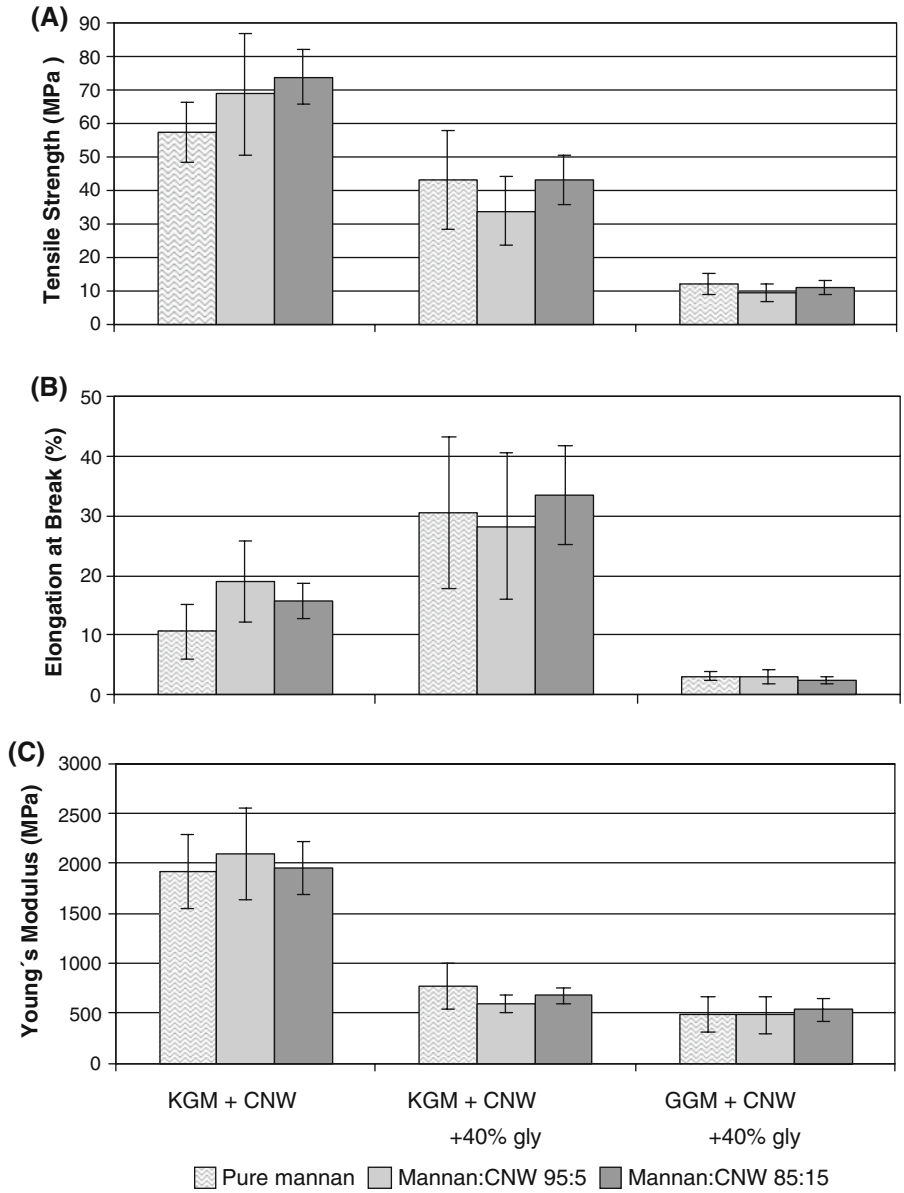

Fig. 8 **a** Tensile strength, (**b**) elongation at break, and (**c**) Young′s modulus of films from KGM and GGM and of composites at KGM:CNW and GGM:CNW weight ratios of 95:5 and 85:15. The GGM-based films contained 40% (wt% of GGM and CNW) glycerol (gly) as plasticizer. The KGM-based films were tested with and without glycerol. The results are averages from 10 to 13 measurements and the *error bars* indicate standard deviations

stability of the glycerol-plasticized KGM- and GGM-based films increased only slightly when CNW was added at the mannan:CNW ratio of 95:5, and somewhat decreased at the ratio of 85:15. The addition of CNW did not significantly affect the E′, E″ or tangent delta of the films. The tensile strength of the KGM-based films increased with increasing amount of CNW when glycerol was not used, but that of glycerol-plasticized KGM- and GGM-based films did not change significantly due to the addition of CNW. The films were rather heterogeneous and therefore the standard deviations in the tensile testing were large. Similarly as in the present study, the reinforcing effect of nanofibrils

on cassava starch matrix was limited (Teixeira et al. 2009).

Regarding the mechanical strength and stiffness of the films, at least three explanations for the lack of larger effect can be considered: (1) the CNW were heterogeneously dispersed in the films, (2) the fibrous and rodlike structures induced by the CNW had low mechanical strength, or (3) the interaction between these structures and the film matrix was weak. In all cases, the major continuous and presumably amorphous film matrix would have been responsible for the mechanical strength of the films. Glycerol and/or water could have attached to the interface of the crystallites and the amorphous film matrix, lubricating the interfacial area and reducing the load transfer between these components. The increase in tensile strength with increasing CNW content in those KGM-based films not containing glycerol supports this reasoning. Unfortunately, GGM does not form cohesive films without an external plasticizer and thus the difference noted with KGM could not be verified with GGM. In addition, the similar temperature of relaxation of the amorphous phases of the films, as shown by DMA, indicates that the degree of plasticization by water and glycerol in that phase did not change when a relatively low amount (5 and 15%) of CNW were added, which also supports the idea that some water and glycerol was located either inside or on the surface of the fibrous and rodlike structures as well as in the main film matrix. All GGM films as well as plasticized KGM films with different CNW content were equally easy to handle indicating similar plasticizer level in the matrix. This would also be in agreement with a study of starch-CNW composites by Anglès and Dufresne (2000), who concluded that glycerol accumulated in the amylopectin-cellulose interface. To reduce the interference of glycerol during film preparation, we first mixed the mannans and CNW in water and after that added the glycerol. The formation of the fibrous and rodlike structures could have occurred during mixing of the film solution, and when added afterwards, the glycerol could have attached to the surface of these structures. An experiment was conducted by mixing KGM and CNW in water containing glycerol, and noting the formation of fibrous structures similar to those described earlier in this report.

Mathew et al. (2008) showed that the mechanical performance of the starch-CNW composites was higher with sorbitol as plasticizer instead of glycerol and illustrated this with formation of a rigid network of sorbitol, amylopectin, and CNW. Additionally, higher filler loads than those used in the present study had a notable reinforcing effect on the starch-based films (Lu et al. 2006). In the present work, the CNW were apparently heterogenously dispersed in the film matrix as detected by the film appearance. Feasible explanation for the formed structures is strong interactions between mannans and CNW.

Conclusions

Mannans and CNW showed interactions seen as the formation of fiberlike structures with lengths of several millimeters in KGM-CNW composite films, and rodlike structures with lengths of tens of micrometers in GGM-CNW composite films. The differences in the degree of crystallinity of mannans due to the addition of CNW were small and did not correspond to the remarkable differences in the visual appearance of the films. In contrast, mannans could gather CNW into larger visible structures. The tensile strength of unplasticized KGM films increased with increasing CNW content, but unexpectedly the mechanical properties of the plasticized films were not affected by the addition of CNW, most probably due to accumulation of glycerol in the CNW-matrix interface. DMA showed similar plasticization of the film matrix regardless of the amount of CNW, confirming that some glycerol was located in the interface. To our knowledge, this is the first report on mannan-CNW composite films and we are not aware of other studies with CNW showing similar interaction with other plant-derived polysacchairdes, such as starch or xylan. The interactions of plant cell-wall polysaccharides in composite materials should indeed be studied more in future. Even though the mechanical properties of the films were not affected by the addition of CNW, the barrier properties could be an interesting subject for further studies.

Acknowledgments We thank the Laboratory of Polymer Chemistry of the University of Helsinki for use of the dynamic mechanical analyzer and Mikko Karesoja for kind assistance. Marko Peura is acknowledged for his contribution to the X-ray study. The Foundation for Natural Resources in Finland, the Nordic Forest Research Co-operation Committee, and the Academy of Finland are acknowledged for financial support.

References

Anglès MN, Dufresne A (2000) Plasticized starch/tunicin whiskers nanocomposite materials. 1. Structural analysis. Macromolecules 33:8344–8353

Anglès MN, Dufresne A (2001) Plasticized starch/tunicin whiskers nanocomposite materials. 2. Mechanical behavior. Macromolecules 34:2921–2931

Atkins EDT, Farnell S, Mackie W, Sheldrick B (1988) Crystalline structure and packing of mannan I. Biopolymers 27:1097–1105

Bondenson D, Mathew A, Oksman K (2006) Optimization of the isolation of nanocrystals from microcrystalline cellulose by acid hydrolysis. Cellulose 13:171–180

Chanzy HD, Grosrenaud A, Joseleau JP, Dubé M, Marchessault RH (1982) Crystallization behavior of glucomannan. Biopolymers 21:301–319

Cheng LH, Karim AA, Seow CC (2006) Effects of water-glycerol and water-sorbitol interactions on the physical properties of konjac glucomannan films. J Food Sci 71:E62–E67

de Souza Lima MM, Borsali R (2004) Rodlike cellulose microcrystals: structure, properties, and applications. Macromol Rapid Commun 25:771–787

Guinier A (1994) X-ray diffraction in crystals, imperfect crystals, and amorphous bodies. Dover publications Inc, New York

Hartman J, Albertsson A-C, Söderqvist Lindblad M, Sjöberg J (2006) Oxygen barrier materials from renewable sources: material properties of softwood hemicellulose-based films. J Appl Polym Sci 100:2985–2991

Kraus W, Nolze GJ (1996) POWDER CELL—A program for the representation and manipulation of crystal structures and calculation of the resulting X-ray powder patterns. J Appl Crystallogr 29:301–303

Kvien I, Sugiyama J, Votrubec M, Oksman K (2007) Characterization of starch based nanocomposites. J Mater Sci 42:8163–8171

Laine P, Lampi A-M, Peura M, Kansikas J, Mikkonen KS, Willför S, Tenkanen M, Jouppila K Comparison of microencapsulation properties of Spruce (*Picea abies*) Galactoglucomannan and Gum Arabic (submitted)

Li B, Xie B, Kennedy JF (2006a) Studies on the molecular chain morphology of konjac glucomannan. Carbohydr Polym 64:510–515

Li B, Kennedy JF, Jiang QG, Xie BJ (2006b) Quick dissolvable, edible and heatsealable blend films based on konjac glucomannan—gelatin. Food Res Int 39:544–549

Lu Y, Weng L, Cao X (2006) Morphological, thermal and mechanical properties of ramie crystallites—reinforced plasticized starch biocomposites. Carbohydr Polym 63:198–204

Mathew AP, Thielemans W, Dufresne A (2008) Mechanical properties of nanocomposites from sorbitol plasticized starch and tunicin whiskers. J Appl Polym Sci 109:4065–4074

McHugh TH, Krochta JM (1994) Permeability properties of edible films. In: Krochta JM, Baldwin EA, Nisperos-Carriedo M (eds) Edible coatings and films to improve food quality. Technomic Publishing Company, Lancaster, pp 139–183

Mikkonen KS, Rita H, Helén H, Talja RA, Hyvönen L, Tenkanen M (2007) Effect of polysaccharide structure on mechanical and thermal properties of galactomannan-based films. Biomacromolecules 8:3198–3205

Mikkonen KS, Yadav MP, Cooke P, Willför S, Hicks KB, Tenkanen M (2008) Films from spruce galactoglucomannan blended with poly(vinyl alcohol), corn arabinoxylan, and konjac glucomannan. BioRes 3:178–191

Nordqvist D, Idermark J, Hedenqvist MS, Gällstedt M, Ankerfors M, Lindström T (2007) Enhancement of the wet properties of transparent chitosan-acetic-acid-salt films using microfibrillated cellulose. Biomacromolecules 8:2398–2403

Persson T, Nordin A-K, Zacchi G, Jönsson A-S (2007) Economic evaluation of isolation of hemicelluloses from process streams from thermomechanical pulping of spruce. Appl Biochem Biotechnol 136–140:741–752

Petersson L, Kvien I, Oksman K (2007) Structure and thermal properties of poly(lactic acid)/cellulose whiskers nanocomposite materials. Composites Sci Technol 67:2535–2544

Samir MASA, Alloin F, Dufresne A (2005) Review of recent research into cellulosic whiskers, their properties and their application in nanocomposite field. Biomacromolecules 6:612–626

Saxena A, Elder TJ, Pan S, Ragauskas AJ (2009) Novel nanocellulosic xylan composite film. Composites: Part B 40:727–730

Sjöström E (1993) Wood chemistry fundamentals and applications. Academic Press Inc, San Diego

Sorrentino A, Gorrasi G, Vittoria V (2007) Potential perspectives of bio-nanocomposites for food packaging applications. Trends Food Sci Technol 18:84–95

Takigami S (2000) Konjac Mannan. In: Phillips GO, Williams PA (eds) Handbook of hydrocolloids. Woodhead Publishing, Cambridge, UK

Teixeira EM, Pasquini D, Curvelo AAS, Corradini E, Belgacem MN, Dufresne A (2009) Cassava bagasse cellulose nanofibrils reinforced thermoplastic cassava starch. Carbohydr Polym 78:422–431

Willför S, Rehn P, Sundberg A, Sundberg K, Holmbom B (2003) Recovery of water-soluble acetylgalactoglucomannans from mechanical pulp of spruce. Tappi J 2:27–32

Willför S, Sundberg K, Tenkanen M, Holmbom B (2008) Spruce-derived mannans—A potential raw material for hydrocolloids and novel advanced natural materials. Carbohydr Polym 72:197–210

Xiao C, Lu Y, Liu H, Zhang L (2001) Preparation and characterization of konjac glucomannan and sodium carboxymethylcellulose blend films. J Appl Polym Sci 80:26–31

Xu C, Willför S, Holmlund P, Holmbom B (2009) Rheological properties of water-soluble spruce O-acetyl galactoglucomannans. Carbohydr Polym 75:498–504